

This article was downloaded by:

On: 23 January 2011

Access details: *Access Details: Free Access*

Publisher *Taylor & Francis*

Informa Ltd Registered in England and Wales Registered Number: 1072954 Registered office: Mortimer House, 37-41 Mortimer Street, London W1T 3JH, UK



## Journal of Coordination Chemistry

Publication details, including instructions for authors and subscription information:

<http://www.informaworld.com/smpp/title~content=t713455674>

### A transition-metal-templated 3-D supramolecular framework based on molybdenum-vanadium polyoxoanions

Yu-Kun Lu<sup>ab</sup>; Xiao-Bing Cui<sup>a</sup>; Jia-Ning Xu<sup>a</sup>; Qian Gao<sup>a</sup>; Yan Chen<sup>a</sup>; Juan Jin<sup>a</sup>; Shu-Yun Shi<sup>a</sup>; Ji-Qing Xu<sup>a</sup>; Tie-Gang Wang<sup>a</sup>

<sup>a</sup> College of Chemistry and State Key Laboratory of Inorganic Synthesis and Preparative Chemistry, Jilin University, Changchun, Jilin 130021, P.R. China <sup>b</sup> College of Chemistry and Chemical Engineering, China University of Petroleum (East China), Qingdao Shandong 266555, P.R. China

First published on: 19 January 2010

**To cite this Article** Lu, Yu-Kun , Cui, Xiao-Bing , Xu, Jia-Ning , Gao, Qian , Chen, Yan , Jin, Juan , Shi, Shu-Yun , Xu, Ji-Qing and Wang, Tie-Gang(2010) 'A transition-metal-templated 3-D supramolecular framework based on molybdenum-vanadium polyoxoanions', *Journal of Coordination Chemistry*, 63: 3, 394 – 405, First published on: 19 January 2010 (iFirst)

**To link to this Article:** DOI: 10.1080/00958970903469704

**URL:** <http://dx.doi.org/10.1080/00958970903469704>

PLEASE SCROLL DOWN FOR ARTICLE

Full terms and conditions of use: <http://www.informaworld.com/terms-and-conditions-of-access.pdf>

This article may be used for research, teaching and private study purposes. Any substantial or systematic reproduction, re-distribution, re-selling, loan or sub-licensing, systematic supply or distribution in any form to anyone is expressly forbidden.

The publisher does not give any warranty express or implied or make any representation that the contents will be complete or accurate or up to date. The accuracy of any instructions, formulae and drug doses should be independently verified with primary sources. The publisher shall not be liable for any loss, actions, claims, proceedings, demand or costs or damages whatsoever or howsoever caused arising directly or indirectly in connection with or arising out of the use of this material.

## A transition-metal-templated 3-D supramolecular framework based on molybdenum–vanadium polyoxoanions

YU-KUN LU<sup>†‡</sup>, XIAO-BING CUI<sup>†</sup>, JIA-NING XU<sup>†</sup>, QIAN GAO<sup>†</sup>, YAN CHEN<sup>†</sup>,  
JUAN JIN<sup>†</sup>, SHU-YUN SHI<sup>†</sup>, JI-QING XU<sup>\*†</sup> and TIE-GANG WANG<sup>†</sup>

<sup>†</sup>College of Chemistry and State Key Laboratory of Inorganic Synthesis and Preparative Chemistry, Jilin University, Changchun, Jilin 130021, P.R. China

<sup>‡</sup>College of Chemistry and Chemical Engineering, China University of Petroleum (East China), Qingdao Shandong 266555, P.R. China

(Received 25 June 2009; in final form 14 August 2009)

A polyoxometalate [Co(phen)<sub>3</sub>][Co(en)<sub>3</sub>][Co(en)<sub>2</sub>(H<sub>2</sub>O)<sub>2</sub>][Co(en)<sub>2</sub>]<sub>0.5</sub>[PMo<sub>8</sub><sup>VI</sup>V<sub>4</sub><sup>VO</sup>O<sub>40</sub>(V<sup>IV</sup>O)<sub>2</sub>]·6H<sub>2</sub>O (**1**) (en = ethylenediamine, phen = 1,10-phenanthroline) has been hydrothermally synthesized and structurally characterized by single-crystal X-ray diffraction, IR, electron paramagnetic resonance, X-ray photoelectron spectroscopy, elemental analyses, and thermogravimetry. The structure is an interesting 3-D supramolecular network containing bi-capped Keggin-type molybdenum–vanadium clusters with transition metal complexes generated *in situ* under mild hydrothermal conditions. Compound **1** contains four different counteractions being coordinated complexes of cobalt. The magnetic properties of **1** have also been studied in the temperature range of 4–300 K, and its magnetic susceptibility obeys the Curie–Weiss law, showing ferromagnetic coupling.

**Keywords:** Polyoxometalates; *In situ* template; Supramolecular; Magnetic property

### 1. Introduction

Crystal engineering is an important emerging area of research to obtain crystals with various structures and functionalities for applications such as sorption media and catalysts [1–4]. Supramolecular chemistry has developed at a tremendous rate [5]. In the construction of supramolecular materials, a strategy is to extend low-dimensional building blocks to high-dimensional networks through intermolecular interactions, including hydrogen bonding,  $\pi \cdots \pi$  stacking, Van der Waals interactions, etc. [6]; the hydrogen bond is the most familiar organizing force in supramolecular assemblies by the virtue of its unique strength and directionality that may control short-range packing [7].

In the design of supramolecular materials, it is important to choose suitable building blocks to exploit organic substrates with structure-directing properties [8]. An attractive building block is polyoxometalate (POM) clusters due to their structural diversity and many oxygen atoms on spherical surface [9]. Recent promising approach toward the synthesis lies in the selection of POMs as building blocks and organic moieties as structure-directing agents [8, 10–14]. In order to study the structure of supramolecules

\*Corresponding author. Email: xjq@mail.jlu.edu.cn

with large template, transition metal complexes (TMCs) possessing relatively large volumes and complicated cation structures were introduced in the reaction system. To the best of our knowledge, there are only limited reports about TMCs as templates or structure-directing agents, and the relationship between POMs and TMCs has been infrequently studied [15–17].

To increase the negative charge density of heteropolymolybdates [18–28], we substituted  $\text{Mo}^{\text{VI}}$  with lower-valence  $\text{V}^{\text{IV}}$  [29–33]. To expand molybdenum–vanadium POMs [34, 35], we recently focused on Mo–V clusters as structural building blocks in the syntheses of hydrogen-bonded high-dimensional structures templated by TMCs.

In this article, we report a TMCs-templated 3-D supramolecular network based on Mo–V clusters,  $[\text{Co}(\text{phen})_3][\text{Co}(\text{en})_3][\text{Co}(\text{en})_2(\text{H}_2\text{O})_2][\text{Co}(\text{en})_2]_{0.5}[\text{PMo}_8\text{V}_6\text{O}_{42}] \cdot 6\text{H}_2\text{O}$  (**1**) (en = ethylenediamine, phen = 1,10-phenanthroline). Compound **1** contains four different coordination complexes of Co. Based on reduced polyoxoanion  $[\text{PMo}_8\text{V}_6\text{O}_{42}]^{7-}$ , an interesting hydrogen-bonded host network is formed and employed to accommodate the TMCs templates. We also discuss the formation of **1** and the function of each TMC fragment in crystallization.

## 2. Experimental

### 2.1. Material and methods

All chemicals purchased were of reagent grade and used without purification. Inductively coupled plasma (ICP) analysis was conducted on a Perkin-Elmer Optima 3300 DV spectrometer. Elemental analysis (C, H, and N) was performed on a Perkin-Elmer 2400 CHN Elemental Analyzer. IR (KBr pellets) spectra were recorded from 450 to 4000  $\text{cm}^{-1}$  using a Perkin-Elmer Spectrum One spectrophotometer. Electron paramagnetic resonance (EPR) was carried out on a Bruker ER 200D-SRC spectrometer at 298 K. X-ray photoelectron spectroscopy (XPS) was performed on a Thermo ESCALAB 250 spectrometer with a Mg-K $\alpha$  (1253.6 eV) achromatic X-ray source. Thermogravimetric analysis (TGA) was carried out on a Perkin-Elmer TAG-7 instrument from room temperature to 800°C with a heating rate of 10°C  $\text{min}^{-1}$ . Temperature-dependent magnetic susceptibility for **1** was recorded on a Quantum Design MPMS XL-5 SQUID magnetometer under an applied field of 1000 Oe from 4 to 300 K.

### 2.2. Synthesis of $[\text{Co}(\text{phen})_3][\text{Co}(\text{en})_3][\text{Co}(\text{en})_2(\text{H}_2\text{O})_2][\text{Co}(\text{en})_2]_{0.5}[\text{PMo}_8^{\text{VI}}\text{V}_4^{\text{IV}}\text{O}_{40}(\text{V}^{\text{IV}}\text{O})_2] \cdot 6\text{H}_2\text{O}$ (**1**)

A mixture of  $\text{KH}_2\text{PO}_4 \cdot 2\text{H}_2\text{O}$  (0.7 g, 0.5 mmol),  $(\text{NH}_4)_6\text{Mo}_7\text{O}_{24} \cdot 4\text{H}_2\text{O}$  (0.71 g, 0.57 mmol),  $\text{VOSO}_4 \cdot 2\text{H}_2\text{O}$  (0.80 g, 4 mmol),  $\text{CoCl}_2 \cdot 2\text{H}_2\text{O}$  (0.60 g, 2.5 mmol), phen (0.50 g, 2.5 mmol), and  $\text{H}_2\text{O}$  (20 mL) was mixed, stirred for 30 min, and the pH was adjusted to 8 with en. The resulting suspension was transferred to a Teflon-lined autoclave (25 mL) and kept at 180°C for 3 days. After cooling gradually to room temperature for 2 days, black prism crystals were obtained by filtering, washing with distilled water, and drying in a desiccator at ambient temperature. The yield was 47% based on Mo. Elemental Anal. Calcd (%) for **1**:  $\text{C}_{48}\text{H}_{88}\text{Co}_{3.50}\text{Mo}_8\text{N}_{18}\text{O}_{50}\text{PV}_6$

(3027.75): C, 19.41; H, 2.93; N, 8.33; Co, 6.81; Mo, 25.35; V, 10.09; P, 1.02. Found (%): C, 19.26; H, 3.01; N, 8.29; Co, 6.92; Mo, 25.19; V, 10.38; P, 1.09.

### 2.3. X-ray crystallography

The crystal structure was determined by single-crystal X-ray diffraction analysis. The data were collected on a Bruker-AXS Smart CCD diffractometer (Mo-K $\alpha$ ,  $\lambda = 0.71073 \text{ \AA}$ ) at room temperature with  $\omega$ -scan mode. Empirical absorption corrections were applied. The structure was solved by direct methods and refined by full-matrix least squares on  $F^2$  using SHELXTL-6.10 [36]. All non-hydrogen atoms were refined anisotropically except for C-37 and C-42. A summary of crystal data and structure refinement for **1** is provided in table 1. Selected bond lengths of **1** are listed in table 2. Some hydrogen bonding data is listed in table S1.

## 3. Results and discussion

### 3.1. Synthesis

Compound **1** was prepared with good yield through hydrothermal reaction at pH 8. The hydrothermal method is effective for syntheses of POMs [37, 38]. Small changes in one or more of reaction factors, such as pH value [39], temperature [40], reaction time, molar ratio of the reactants, etc., may have profound influence on final reaction products. The pH is crucial for formation of **1**; no compound was obtained when pH is more than 8.5 or less than 7.5. To study the structure of POMs with TMCs possessing different volumes, we selected two ligands, phen and en. When other reaction

Table 1. The crystallographic data for **1**.

|  |  |
|--|--|
| Compound   | <b>1</b>   |
| Empirical formula  | C <sub>48</sub> H <sub>88</sub> Co <sub>3.50</sub> Mo <sub>8</sub> N <sub>18</sub> O <sub>50</sub> PV <sub>6</sub> |
| Formula weight   | 3027.75  |
| Crystal system   | Monoclinic   |
| Space group  | $P2_1/n$   |
| Unit cell dimensions ( $\text{\AA}$ , $^\circ$ )         |  |
| <i>a</i>   | 24.094(5)  |
| <i>b</i>   | 13.219(3)  |
| <i>c</i>   | 28.505(6)  |
| $\beta$  | 94.22(3)   |
| Volume ( $\text{\AA}^3$ ), <i>Z</i>                      | 9054(3), 4   |
| Calculated density ( $\text{g cm}^{-3}$ )                | 2.221  |
| Absorption coefficient ( $\text{mm}^{-1}$ )              | 2.396  |
| $F(000)$   | 5942   |
| $\theta$ range for data collection ( $^\circ$ )          | 2.10–26.11   |
| Limiting indices   | $-29 \leq h \leq 29$ ; $-16 \leq k \leq 16$ ; $-35 \leq l \leq 35$   |
| Reflections collected/unique                             | 76,419/17,976 [ $R(\text{int}) = 0.0452$ ]   |
| Completeness to $\theta$ (%)                             | 99.8   |
| Data/restraints/parameters                               | 17976/0/1203   |
| Goodness-of-fit on $F^2$                                 | 1.035  |
| Final <i>R</i> indices [ $I > 2\sigma(I)$ ]              | $R_1 = 0.0380$ , $wR_2 = 0.0955$   |
| <i>R</i> indices (all data) <sup>a</sup>                 | $R_1 = 0.0519$ , $wR_2 = 0.1027$   |
| Largest difference peak and hole ( $\text{e \AA}^{-3}$ ) | 1.573 and $-0.938$   |

<sup>a</sup>  $R_1 = \sum ||F_o| - |F_c|| / \sum |F_o|$ ;  $wR = [\sum w(F_o^2 - F_c^2)^2 / \sum w(F_o^2)^2]^{1/2}$ .

Table 2. Selected bond lengths (Å) for **1**.

|             |          |             |          |               |           |
|-------------|----------|-------------|----------|---------------|-----------|
| P(1)–O(42)  | 1.532(3) | Mo(6)–O(38) | 1.805(3) | V(4)–O(20)    | 1.956(4)  |
| P(1)–O(41)  | 1.538(3) | Mo(6)–O(37) | 1.821(3) | V(4)–O(24)    | 1.970(3)  |
| P(1)–O(39)  | 1.538(3) | Mo(6)–O(34) | 2.048(3) | V(5)–O(13)    | 1.627(3)  |
| P(1)–O(40)  | 1.543(3) | Mo(6)–O(27) | 2.064(3) | V(5)–O(22)    | 1.891(3)  |
| Mo(1)–O(1)  | 1.710(3) | Mo(6)–O(41) | 2.447(3) | V(5)–O(15)    | 1.911(3)  |
| Mo(1)–O(18) | 1.796(3) | Mo(7)–O(7)  | 1.700(3) | V(5)–O(16)    | 1.976(3)  |
| Mo(1)–O(17) | 1.806(3) | Mo(7)–O(35) | 1.797(3) | V(5)–O(19)    | 1.980(3)  |
| Mo(1)–O(16) | 2.050(3) | Mo(7)–O(36) | 1.805(3) | V(6)–O(14)    | 1.626(4)  |
| Mo(1)–O(15) | 2.065(3) | Mo(7)–O(31) | 2.052(3) | V(6)–O(28)    | 1.897(3)  |
| Mo(1)–O(39) | 2.447(3) | Mo(7)–O(34) | 2.076(3) | V(6)–O(34)    | 1.901(3)  |
| Mo(2)–O(2)  | 1.695(3) | Mo(7)–O(42) | 2.437(3) | V(6)–O(31)    | 1.966(3)  |
| Mo(2)–O(21) | 1.790(3) | Mo(8)–O(8)  | 1.699(3) | V(6)–O(27)    | 1.974(3)  |
| Mo(2)–O(20) | 1.808(3) | Mo(8)–O(32) | 1.803(3) | Co(1)–N(6)    | 2.078(4)  |
| Mo(2)–O(15) | 2.061(3) | Mo(8)–O(33) | 1.804(3) | Co(1)–N(5)    | 2.081(4)  |
| Mo(2)–O(19) | 2.083(3) | Mo(8)–O(31) | 2.051(3) | Co(1)–N(1)    | 2.084(4)  |
| Mo(2)–O(40) | 2.434(3) | Mo(8)–O(28) | 2.086(3) | Co(1)–N(3)    | 2.090(4)  |
| Mo(3)–O(3)  | 1.697(3) | Mo(8)–O(42) | 2.474(3) | Co(1)–N(2)    | 2.103(4)  |
| Mo(3)–O(23) | 1.791(3) | V(1)–O(9)   | 1.604(3) | Co(1)–N(4)    | 2.103(4)  |
| Mo(3)–O(24) | 1.815(3) | V(1)–O(32)  | 1.942(3) | Co(2)–N(11)   | 2.116(5)  |
| Mo(3)–O(22) | 2.047(3) | V(1)–O(25)  | 1.948(3) | Co(2)–N(12)   | 2.126(5)  |
| Mo(3)–O(19) | 2.067(3) | V(1)–O(36)  | 1.952(3) | Co(2)–N(10)   | 2.126(5)  |
| Mo(3)–O(40) | 2.435(3) | V(1)–O(23)  | 1.958(3) | Co(2)–N(7)    | 2.130(5)  |
| Mo(4)–O(4)  | 1.700(3) | V(2)–O(10)  | 1.613(3) | Co(2)–N(8)    | 2.137(5)  |
| Mo(4)–O(25) | 1.793(3) | V(2)–O(29)  | 1.936(3) | Co(2)–N(9)    | 2.153(5)  |
| Mo(4)–O(26) | 1.811(3) | V(2)–O(33)  | 1.943(3) | Co(3)–N(14)   | 2.048(10) |
| Mo(4)–O(16) | 2.065(3) | V(2)–O(26)  | 1.951(3) | Co(3)–N(16)   | 2.058(6)  |
| Mo(4)–O(22) | 2.068(3) | V(2)–O(17)  | 1.961(3) | Co(3)–N(13)   | 2.078(6)  |
| Mo(4)–O(39) | 2.430(3) | V(3)–O(11)  | 1.597(4) | Co(3)–N(15)   | 2.153(9)  |
| Mo(5)–O(5)  | 1.713(3) | V(3)–O(21)  | 1.942(3) | Co(3)–O(1W)   | 2.164(5)  |
| Mo(5)–O(29) | 1.790(3) | V(3)–O(37)  | 1.947(3) | Co(3)–O(2W)   | 2.164(4)  |
| Mo(5)–O(30) | 1.809(3) | V(3)–O(18)  | 1.947(3) | Co(4)–N(18)#1 | 1.896(8)  |
| Mo(5)–O(27) | 2.052(3) | V(3)–O(30)  | 1.963(3) | Co(4)–N(18)   | 1.896(8)  |
| Mo(5)–O(28) | 2.061(3) | V(4)–O(12)  | 1.603(3) | Co(4)–N(17)#1 | 1.907(7)  |
| Mo(5)–O(41) | 2.460(3) | V(4)–O(38)  | 1.937(4) | Co(4)–N(17)   | 1.907(7)  |
| Mo(6)–O(6)  | 1.693(4) | V(4)–O(35)  | 1.943(3) |               |           |

Symmetry codes for **1**: #1–*x*, –*y*+2, –*z*.

conditions were unchanged, crystal products of **1** were obtained with lower yield when  $\text{VOSO}_4 \cdot 2\text{H}_2\text{O}$  was replaced with  $\text{V}_2\text{O}_5$  or  $\text{NH}_4\text{VO}_3$ . Compound **1** is insoluble in water and common organic solvents (such as methanol, ethanol, ether, DMF, and DMSO), and is decomposed in nitric acid. The compound is stable in atmosphere.

### 3.2. Crystal structure description of **1**

Single crystal X-ray diffraction analysis reveals that **1** consists of a bi-capped  $\alpha$ -Keggin polyoxoanion  $[\text{PMo}_8^{\text{VI}}\text{V}_4^{\text{IV}}\text{O}_{40}(\text{V}^{\text{IV}}\text{O})_2]^{7-}$ , four different counteranions,  $[\text{Co}(1)(\text{phen})_3]^{2+}$ ,  $[\text{Co}(2)(\text{en})_3]^{2+}$ ,  $[\text{Co}(3)(\text{en})_2(\text{H}_2\text{O})_2]^{2+}$ , and  $[\text{Co}(4)(\text{en})_2]^{2+}$ , and six lattice water molecules. As shown in figure 1, the polyoxoanion  $[\text{PMo}_8^{\text{VI}}\text{V}_4^{\text{IV}}\text{O}_{40}(\text{V}^{\text{IV}}\text{O})_2]^{7-}$  can be described as an  $\alpha$ -Keggin core  $[\text{PMo}_8\text{V}_4\text{O}_{40}]$  with two additional five-coordinate terminal  $\{\text{VO}\}^{2+}$  units capping two opposite  $\{\text{Mo}_4\text{O}_4\}$  square holes and contains a distorted  $\{\text{PO}_4\}$  tetrahedron in the center. The P–O distances are in the usual range of 1.532(3)–1.543(3) Å and P–O–P bond angles vary from 108.79(17) to 110.74(18)°. In the  $\alpha$ -Keggin core  $[\text{PMo}_8\text{V}_4\text{O}_{40}]$ , four  $\{\text{MoO}_6\}$  octahedra form a  $\{\text{Mo}_4\text{O}_{18}\}$  ring *via* the corner sharing and edge sharing, and the two  $\{\text{Mo}_4\text{O}_{18}\}$  rings

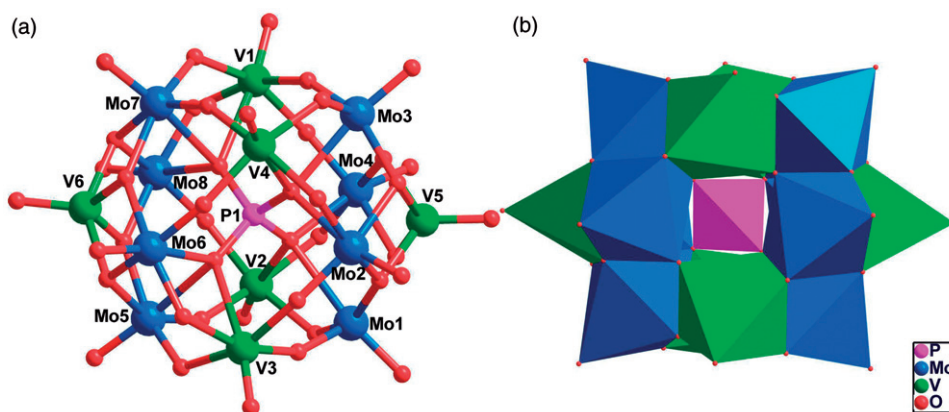


Figure 1. (a) Combined ball-and-stick and (b) polyhedral representation of the polyoxoanion  $[(\text{PO}_4)\text{Mo}_8\text{V}_1\text{V}_4\text{O}_{36}(\text{V}^{\text{IV}}\text{O})_2]^{7-}$  showing the bi-capped  $\alpha$ -Keggin structure.

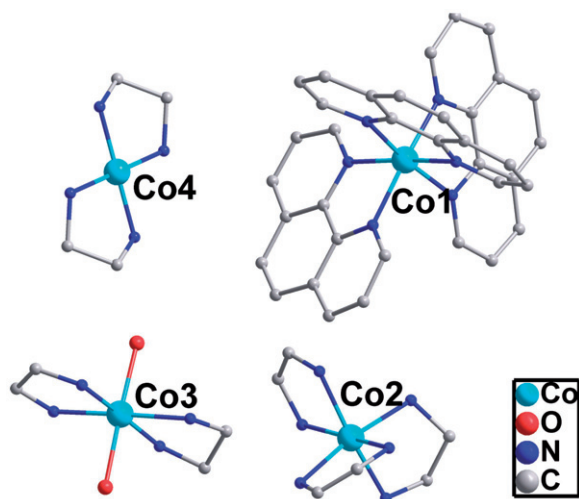


Figure 2. Four different counteranions in **1**.

sandwich four  $\{\text{VO}_5\}$  pyramids through corner sharing. All vanadiums and molybdenums show a distorted  $\{\text{VO}_5\}$  square pyramidal and distorted  $\{\text{MoO}_6\}$  octahedral environment. The Mo/V–O bond distances are divided in three groups: Mo–Oc 2.430(3)–2.474(3) Å (Oc, center O atoms); Mo–Ob 1.790(3)–2.086(3) Å, V–Ob 1.891(3)–1.980(3) Å (Ob, bridge O atoms); and Mo–Ot 1.693(4)–1.713(3) Å, V–Ot 1.597(4)–1.627(3) Å (Ot, terminal O atoms) (table 2). The O–V–O and O–Mo–O bond angles range from 72.76(12)° to 172.92(15)° and from 68.62(11)° to 169.62(15)°, respectively.

There exist four different cobalt complexes, and the Co centers exhibit octahedral and square planar coordination geometries (figure 2). Co-1 is surrounded by six nitrogens from three 1,10-phen ligands with the Co–N distances of 2.078(4)–2.103(4) Å and N–Co–N angles varying from 79.61(17)° to 172.37(17)°; Co-2 is defined by six nitrogens from three en ligands with the Co–N distances of 2.116(5)–2.153(5) Å and

N–Co–N angles in the range of  $80.36(18)^\circ$ – $171.8(2)^\circ$ ; Co-3 is described as a distorted octahedron formed by four nitrogens from two en ligands [ $2.048(10)$ – $2.153(9)$  Å] and two waters [ $2.164(5)$  and  $2.164(4)$  Å]. In contrast to the octahedral coordination geometry of the other three cobalt centers, Co-4 completes its square planar configuration by four nitrogens from two en ligands with the Co–N distances of  $1.896(8)$ – $1.908(7)$  Å and N–Co–N angles in the range of  $86.7(3)^\circ$ – $180.0(4)^\circ$ .

The heteropolyanions are linked by O-3W *via* hydrogen bonding [O-3W  $\cdots$  O-1a,  $2.885(6)$  Å; O-3W  $\cdots$  O-13b,  $2.882(6)$  Å; (a)  $x - 1, y, z$ ; (b)  $1.5 - x, 0.5 + y, 0.5 - z$ .], giving a 1-D infinite supramolecular helical chain with a pitch of  $13.219(3)$  Å along *b* axis (figure 3). Adjacent helical chains are connected by  $[\text{Co}(\text{en})_2(\text{H}_2\text{O})_2]^{2+}$  fragments to form a 2-D supramolecular layered structure along *ab* through hydrogen bonds (figure S1), [O-1W  $\cdots$  O-5,  $2.942(7)$  Å; O-1W  $\cdots$  O-24a,  $2.793(6)$  Å; O-2W  $\cdots$  O-14b,  $2.767(6)$  Å; O-2W  $\cdots$  O-7b,  $2.910(6)$  Å; (a)  $x, 1 + y, z$ ; (b)  $1.5 - x, 0.5 + y, 0.5 - z$ ].  $[\text{Co}(\text{en})_3]^{2+}$  fragments uniformly fill in the holes as templates (figure 4 and table S1).

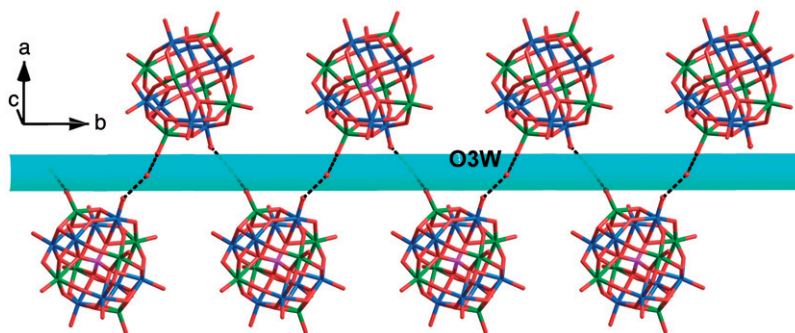


Figure 3. The single-helix chain with a pitch of  $13.219(3)$  Å along the *b* axis in **1**.

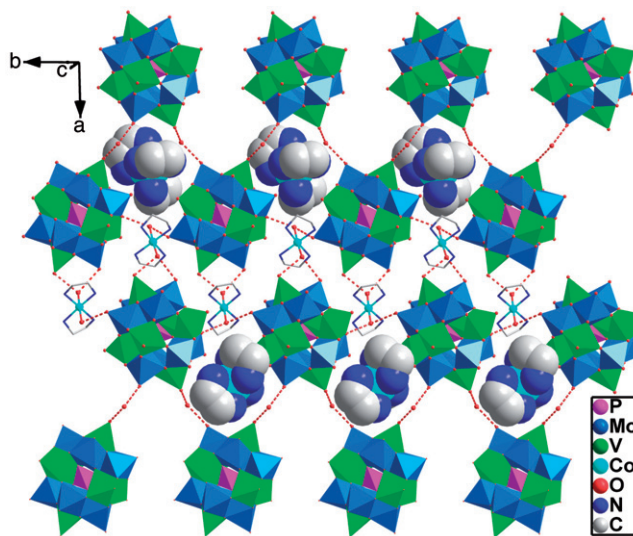


Figure 4. View of the 2-D supramolecular layer of **1** along *c* showing the *in situ* template  $[\text{Co}(\text{en})_3]^{2+}$  as space-filling presentation.

Adjacent supramolecular layers are further connected by  $[\text{Co}(4)(\text{en})_2]^{2+}$  fragments *via* robust hydrogen bonding  $[\text{N}-18 \cdots \text{O}-2$  and  $\text{C}-48 \cdots \text{O}-2]$  with distances of 3.025(8) and 3.250(10) Å, resulting in an interesting host supramolecular network (figure 5a). Each POM center connecting with three  $[\text{Co}(3)(\text{en})_2(\text{H}_2\text{O})_2]^{2+}$  fragments, two O-3W, and one  $[\text{Co}(4)(\text{en})_3]^{2+}$  is viewed as a six-connected node; correspondingly, each  $[\text{Co}(3)(\text{en})_2(\text{H}_2\text{O})_2]^{2+}$  fragment connecting with three POM centers is regarded as a

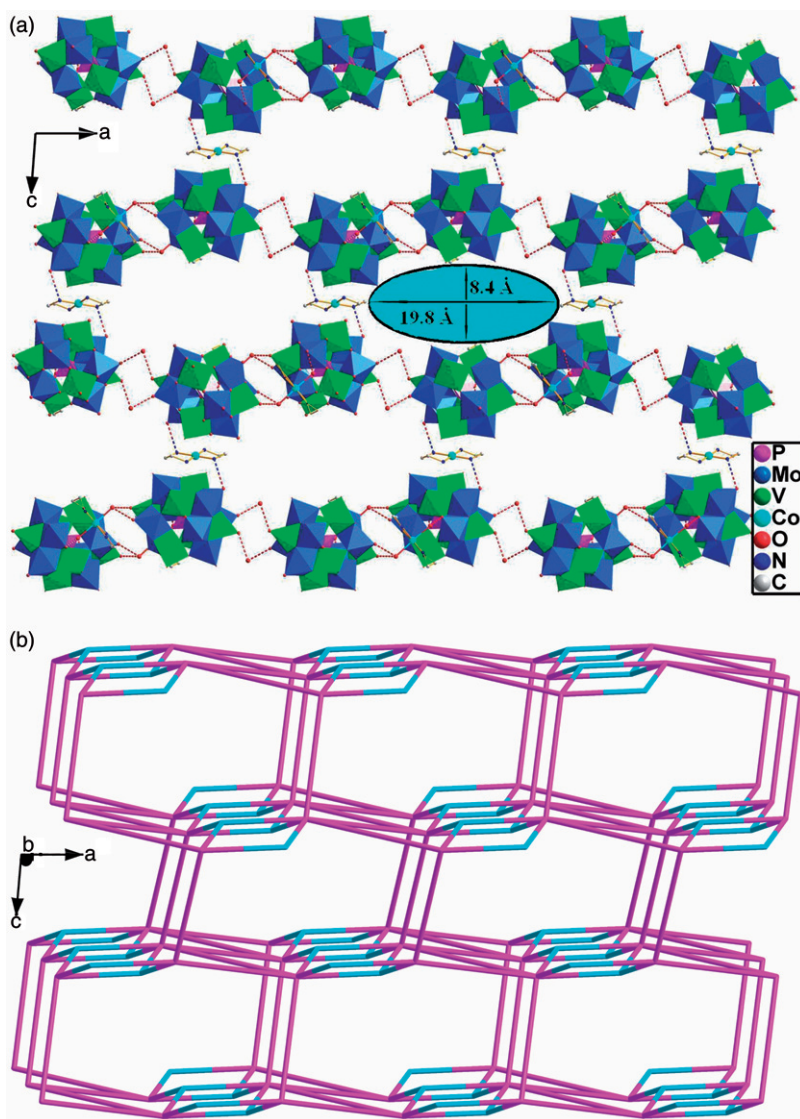


Figure 5. (a) View of the 3-D hydrogen-bonded host supramolecular framework constructed by POM,  $[\text{Co}(\text{en})_2]^{2+}$  and  $[\text{Co}(\text{en})_2(\text{H}_2\text{O})_2]^{2+}$  fragments along the *b* axis and the dimension of channel. (b) Schematic representation of the (3,6)-connected supramolecular topological network with the Schläfli symbol  $(4^3)(4^5 \cdot 6^9 \cdot 8)$  of **1** [six-connected nodes (POMs) are depicted in purple and three-connected nodes ( $[\text{Co}(\text{en})_2(\text{H}_2\text{O})_2]^{2+}$  fragments) in cyan].



three-connected node and the two different kinds of nodes in 1 : 1 ratio interconnect to form a 3-D (3, 6)-connected network with the Schläfli symbol  $(4^3)(4^5 \cdot 6^9 \cdot 8)$  (figure 5b). The most striking feature of the host supramolecular network is that, there exist large channels running along the  $b$  axis. The approximate dimension of the channels is  $8.4 \times 19.8 \text{ \AA}$ . The large volume templates  $[\text{Co}(\text{phen})_3]^{2+}$ , generated *in situ* under mild hydrothermal conditions, are incorporated into the host framework through extensive multipoint C–H $\cdots$ O hydrogen bonding interactions (table S1) with their nearest polyanions (figure 6).

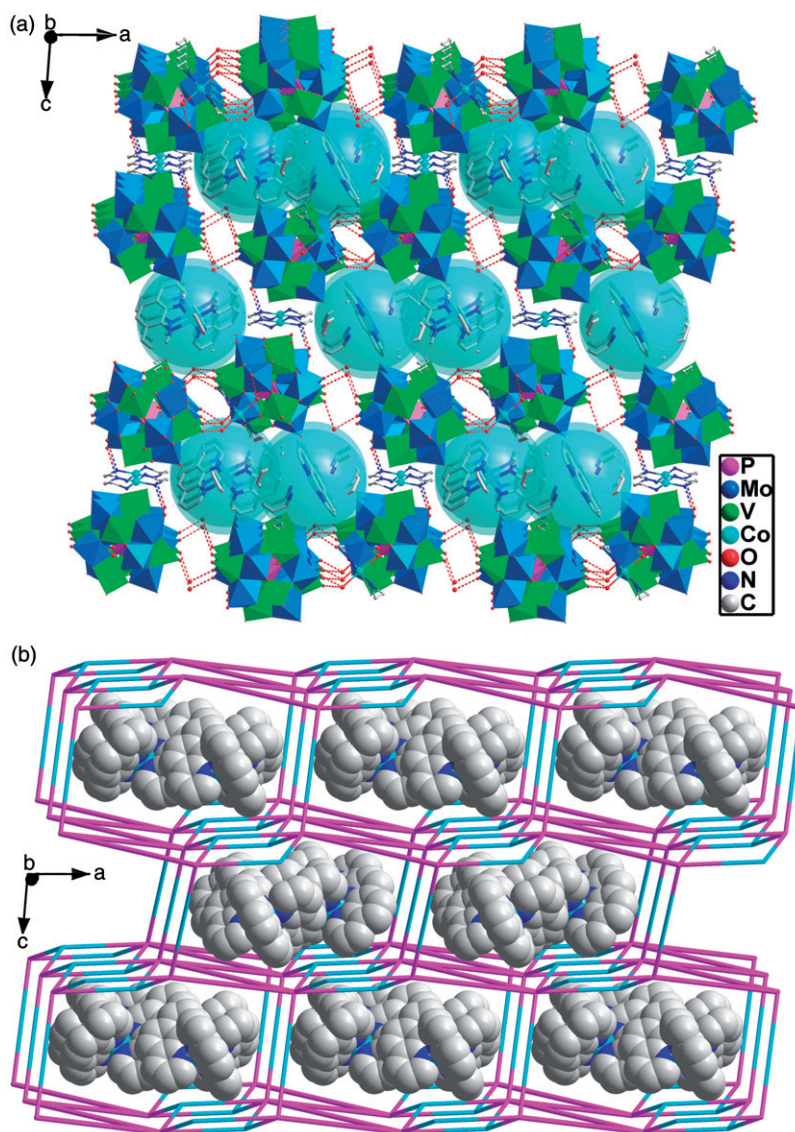


Figure 6. (a) and (b) View of the 3-D host supramolecular framework of **1** along  $b$  showing the guest  $[\text{Co}(\text{phen})_3]^{2+}$  fragments as space filling presentation.

Although the polyoxoanion  $[\text{PMo}_8^{\text{VI}}\text{V}_4^{\text{IV}}\text{O}_{40}(\text{V}^{\text{IV}}\text{O})_2]^{7-}$  has a high negative charge and high nucleophilicity by substituting lower valent  $\text{V}^{\text{IV}}$  for  $\text{Mo}^{\text{VI}}$  [32–35], and the counteraction  $[\text{Co}(4)(\text{en})_2]^{2+}$  possessing unsaturated-coordinated square geometry is a good candidate for linker in the formation of polymer of POMs clusters which have been demonstrated by a large number of facts [32–34], the  $[\text{PMo}_8^{\text{VI}}\text{V}_4^{\text{IV}}\text{O}_{40}(\text{V}^{\text{IV}}\text{O})_2]^{7-}$  units have not been linked *via*  $[\text{Co}(4)(\text{en})_2]^{2+}$  to form an extended structure. We speculate that  $[\text{Co}(1)(\text{phen})_3]^{2+}$  and  $[\text{Co}(2)(\text{en})_3]^{2+}$  with large volumes fill channels preventing  $\text{Co}(4)$  from linking polyoxoanions to generate a high-dimensional covalent structure. The  $[\text{Co}(4)(\text{en})_2]^{2+}$  fragments are restricted in the large spaces constructed by  $[\text{Co}(1)(\text{phen})_3]^{2+}$  fragments and the heteropolyanions, and the shortest distance of  $\text{Co}(4)$  and terminal oxygen of the heteropolyanions is 3.472(4) Å, larger than covalent bonding distance. If the  $[\text{Co}(1)(\text{phen})_3]^{2+}$  and  $[\text{Co}(2)(\text{en})_3]^{2+}$  are absent, the polyanions should be covalently linked through  $[\text{Co}(\text{en})_2]^{2+}$ , and the results have demonstrated our inference [34]. We draw the conclusion that the *in situ* generated  $[\text{Co}(\text{phen})_3]^{2+}$  and  $[\text{Co}(\text{en})_3]^{2+}$  act as structure-directing agents and guests in the construction of **1**.

### 3.3. Characterization of **1**

**3.3.1. Bond valence sum, XPS, and EPR spectrum.** The assignment of oxidation states for the molybdenum and vanadium atoms are consistent with their coordination geometries and are confirmed by valence sum calculations [41] and XPS analysis. The values are 5.92, 5.97, 5.98, 5.93, 5.90, 5.91, 5.93, and 5.90 for Mo(1), Mo(2), Mo(3), Mo(4), Mo(5), Mo(6), Mo(7), and Mo(8), respectively, with an average of 5.93; the calculated valence sums for V(1), V(2), V(3), V(4), V(5), and V(6) are 4.09, 4.05, 4.13, 4.06, 4.05, and 4.08, respectively, with an average of 4.08. The calculated results indicate that all Mo centers are in the +6 oxidation state and all V centers are in the +4 oxidation state.

The XPS for **1** (Supplementary material) shows a peak at 515.8 eV attributed to  $\text{V}^{\text{IV}}2p_{3/2}$ , at 780.1 eV ascribed to  $\text{Co}^{\text{II}}2p_{3/2}$ , along with two peaks at 232.0 and 235.0 eV attributed to  $\text{Mo}^{\text{VI}}3d_{5/2}$  and  $\text{Mo}^{\text{VI}}3d_{3/2}$ , respectively [42, 43]. The EPR spectrum of **1** exhibits the  $\text{V}^{4+}$  signal at 293 K with  $g=1.963$  (figure S2). All these results further confirm the structure analysis.

**3.3.2. Infrared spectrum and TGA.** In the IR spectrum for **1** (figure S3), the strong bands at 1034, 960–910, 869–770, and 727–645  $\text{cm}^{-1}$  should be attributed to the vibration modes for  $\nu(\text{P}-\text{O})$ ,  $\nu(\text{M}-\text{Ot})$ ,  $\nu(\text{M}-\text{Ob}-\text{M})$ , and  $\nu(\text{M}-\text{Oc}-\text{M})$  ( $\text{M} = \text{Mo}$  or  $\text{V}$ ), respectively [2, 23, 33]. The broad band of 3315  $\text{cm}^{-1}$  are from coordination and crystallization water; peaks at 3274 and 3156  $\text{cm}^{-1}$  are attributed to stretching vibrations of N–H in en, peak at 3058  $\text{cm}^{-1}$  is due to stretching of C–H in phen, peaks at 2945 and 2881  $\text{cm}^{-1}$  should be attributed to the stretching of  $-\text{CH}_2-$  in en, peaks at 1626, 1583, 1518, and 1426  $\text{cm}^{-1}$  are attributed to the stretching of C=C and C=N bonds of phen, and peaks in the range of 1339–1104  $\text{cm}^{-1}$  are characteristic of C–N bonds in en [23, 33, 44].

TG curve of **1** exhibits three steps of weight losses (Supplementary material). The first weight loss of 3.66% (Calcd weight loss 3.57%) corresponds to the release of six lattice waters below  $\sim 140^\circ\text{C}$ . The second weight loss is 6.95% (Calcd 7.14%) in the

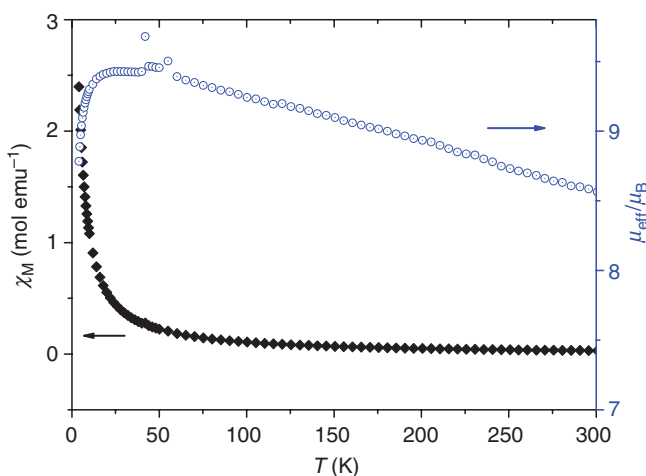


Figure 7. The effective magnetic moment  $\mu_{\text{eff}}$  and molar susceptibility vs. temperature for **1**.

temperature range 280–430°C, corresponding to the decomposition of three en molecules and two coordinated water molecules. The remainder (in the range 470–610°C) are attributed to the decomposition of three en and three phen molecules (Calcd weight loss 23.81%; found 23.26%). The final products are  $\text{MoO}_3$ ,  $\text{V}_2\text{O}_5$ , and  $\text{CoO}$ , and the oxidation of  $\text{V}^{\text{IV}}$  into  $\text{V}^{\text{V}}$  occurred in the process of heating. The whole weight loss (33.87%) is in good agreement with the calculated value (32.94%).

**3.3.3. Magnetic property.** Preliminary magnetic studies have been performed on a crystal sample of **1** from 5 to 300 K. Figure 7 shows the magnetic behavior of **1** in the form of  $\mu_{\text{eff}}$  versus  $T$  and  $\chi_{\text{M}}$  versus  $T$  plots. The room temperature value ( $\mu_{\text{eff}} = 8.56\mu_{\text{B}}$ ) is bigger than expected ( $\mu_{\text{eff}} = 7.64\mu_{\text{B}}$ ) for 2.5 uncoupled  $S = 1/2$  spins of  $\text{Co}^{2+}$ , 1 uncoupled  $S = 3/2$  spins of  $\text{Co}^{2+}$  atoms, and 6 uncoupled  $S = 1/2$  spins of  $\text{V}^{\text{IV}}$  atoms (assuming  $g = 2.68$  for  $\text{Co}^{2+}$  and  $g = 2.00$  for  $\text{V}^{\text{IV}}$ ), indicative of ferromagnetic coupling. Upon cooling, the  $\mu_{\text{eff}}$  continuously increases to a maximum value of  $9.68\mu_{\text{B}}$  at 42 K, indicating the presence of the ferromagnetic exchange interactions. The magnetic data of **1** obey the Curie–Weiss law in the range of 50–300 K, and give values  $C = 9.40 \text{ emu mol}^{-1} \text{ K}$  and  $\theta = 6.20 \text{ K}$ , characteristic of ferromagnetic interactions. Unfortunately, no suitable theoretical model is available in the literature [45] for such a complex system.

#### 4. Conclusion

We have synthesized and characterized a TMCs-templated 3-D supramolecular network based on polyoxoanions. The 3-D supramolecular network contains bi-capped Keggin-type Mo–V clusters and templated TMC generated *in situ* under mild hydrothermal conditions. Furthermore, we discussed the formation and the function of each component in the crystallization process. The magnetic susceptibility of **1** obeys

the Curie–Weiss law, showing ferromagnetic coupling. In order to understand and master the influences of different ligands and transition-metal centers constructing *in situ* templates on the structures and performances of synthesized POMs-based compounds, further relevant research is underway in our group.

## Supplementary material

CCDC number 733428 contains the supplementary crystallographic data for **1**. These data can be obtained free of charge *via* <http://www.ccdc.cam.ac.uk/conts/retrieving.html>, or from the Cambridge Crystallographic Data Centre, 12 Union Road, Cambridge CB2 1EZ, UK; Fax: (+44) 1223-336-033; or Email: [deposit@ccdc.cam.ac.uk](mailto:deposit@ccdc.cam.ac.uk). Selected bond lengths (Å) and angles (°) of N(C)–H···O hydrogen bonding for **1**; view of 2-D supramolecular-layered structure constructed from single-helix chains and [Co(en)<sub>2</sub>(H<sub>2</sub>O)<sub>2</sub>]<sup>2+</sup> fragments through hydrogen bonding in **1**; EPR spectrum of **1**; IR spectrum of **1**; XPS for Mo, V, and Co in **1**; thermogravimetric pattern for **1**.

## Acknowledgments

This work was supported by the National Natural Science Foundation of China (Grant No. 20571032).

## References

- [1] C.L. Hill. *Chem. Rev.*, **98**, 1 (1998).
- [2] M.T. Pope. *Heteropoly and Isopoly Oxometalates*, Springer-Verlag, Berlin (1983).
- [3] V. Soghomonian, Q. Chen, R.C. Haushalter, J. Zubieta. *Science*, **259**, 1596 (1993).
- [4] O.M. Yaghi, M. O'Keeffe, N.W. Ockwig, H.K. Chae, M. Eddaoudi, J. Kim. *Nature*, **423**, 705 (2003).
- [5] J.M. Lehn. *Comprehensive Supramolecular Chemistry*, Pergamon, New York (1996).
- [6] C.N.R. Rao, S. Natarajan, R. Vaidhyanathan. *Angew. Chem. Int. Ed.*, **43**, 1466 (2004).
- [7] S.V. Kolotuchin, E.E. Fenlon, S.R. Wilson, C.J. Loweth, S.C. Zimmerman. *Angew. Chem. Int. Ed.*, **34**, 2654 (1995).
- [8] T. Akutagawa, D. Endo, S.I. Noro, L. Cronin, T. Nakamura. *Coord. Chem. Rev.*, **251**, 2547 (2007).
- [9] M.T. Pope, A. Müller. *Angew. Chem. Int. Ed.*, **30**, 34 (1991).
- [10] C. Streb, D.L. Long, L. Cronin. *Cryst. Eng. Commun.*, **8**, 629 (2006).
- [11] Y.M. Xie, Q.S. Zhang, Z.G. Zhao, X.Y. Wu, S.C. Chen, C.Z. Lu. *Inorg. Chem.*, **47**, 8086 (2008).
- [12] M.L. Wei, C. He, W.J. Hua, C.Y. Duan, S.H. Li, Q.J. Meng. *J. Am. Chem. Soc.*, **128**, 13318 (2006).
- [13] J.P. Wang, S.Z. Li, J.Y. Niu. *J. Coord. Chem.*, **60**, 1327 (2007).
- [14] J. Li, Y.F. Qi, E.B. Wang, J. Li, H.F. Wang, Y.G. Li, Y. Lu, N. Hao, L. Xu, C.W. Hu. *J. Coord. Chem.*, **57**, 715 (2004).
- [15] G.M. Wang, Y.Q. Sun, G.Y. Yang. *J. Solid State Chem.*, **179**, 1545 (2006).
- [16] X.Y. Zhao, D.D. Liang, S.X. Liu, C.Y. Sun, R.G. Cao, C.Y. Gao, Y.H. Ren, Z.M. Su. *Inorg. Chem.*, **47**, 7133 (2008).
- [17] Y. Wang, J.H. Yu, M. Guo, R.R. Xu. *Angew. Chem. Int. Ed.*, **42**, 4089 (2003).
- [18] A. Dolbecq, P. Mialane, L. Lisnard, J. Marrot, F. Sécheresse. *Chem. Eur. J.*, **9**, 2914 (2003).
- [19] A. Müller, C. Beugholt, P. Kögerler, H. Bögge, S. Bud'ko, M. Luban. *Inorg. Chem.*, **39**, 5176 (2000).
- [20] X.L. Wang, C. Qin, E.B. Wang, Z.M. Su, Y.G. Li, L. Xu. *Angew. Chem. Int. Ed.*, **45**, 7411 (2006).
- [21] Z.Y. Shi, X.J. Gu, J. Peng, X. Yu, E.B. Wang. *Eur. J. Inorg. Chem.*, 385 (2006).
- [22] J.X. Meng, Y.G. Li, X.L. Wang, E.B. Wang. *J. Coord. Chem.*, **62**, 2283 (2009).

- [23] Q. Chen, C.L. Hill. *Inorg. Chem.*, **35**, 2403 (1996).
- [24] H.L. Chen, Y. Ding, X.X. Xu, E.B. Wang, W.L. Chen, S. Chang, X.L. Wang. *J. Coord. Chem.*, **62**, 347 (2009).
- [25] Q.X. Han, J.P. Wang, J.Y. Niu. *J. Coord. Chem.*, **60**, 1303 (2007).
- [26] H.N. Miras, D.J. Stone, E.J.L. McInnes, R.G. Raptis, P. Baran, G.I. Chilas, M.P. Siquelas, T.A. Kabanos, L. Cronin. *Chem. Commun.*, 4703 (2008).
- [27] M.L. Wei, H.Y. Xu, R.P. Sun. *J. Coord. Chem.*, **62**, 1989 (2009).
- [28] X.J. Wang, X.M. Lu, P.Z. Li, X.H. Pei, C.H. Ye. *J. Coord. Chem.*, **61**, 3753 (2008).
- [29] A. Müller, M. Koop, P. Schiffels, H. Bogge. *J. Chem. Soc., Chem. Commun.*, 1715 (1997).
- [30] Y. Xu, D.R. Zhu, H. Cai, X.Z. You. *Chem. Commun.*, 787 (1999).
- [31] H.B. Liu, Y. Sun, Y.G. Chen, F.X. Meng, D.M. Shi. *J. Coord. Chem.*, **61**, 3102 (2008).
- [32] C.M. Liu, D.Q. Zhang, M. Xiong, D.B. Zhu. *Chem. Commun.*, 1416 (2002).
- [33] Y. Ding, H.L. Chen, E.B. Wang, Y. Ma, X.L. Wang. *J. Coord. Chem.*, **61**, 2347 (2008).
- [34] Y.B. Liu, X.B. Cui, J.Q. Xu, Y.K. Lu, J. Liu, Q.B. Zhang, T.G. Wang. *J. Mol. Struct.*, **825**, 45 (2006).
- [35] L.M. Duan, C.L. Pan, J.Q. Xu, X.B. Cui, F.T. Xie, T.G. Wang. *Eur. J. Inorg. Chem.*, 2578 (2003).
- [36] G.M. Sheldrick. *SHELXL-97, Program Crystal Structure Refinement*, University of Göttingen, Göttingen, Germany (1997).
- [37] S.T. Zheng, H. Zhang, G.Y. Yang. *Angew. Chem., Int. Ed.*, **47**, 3909 (2008).
- [38] J.Y. Niu, P.T. Ma, H.Y. Niu, J. Li, J.W. Zhao, Y. Song, J.P. Wang. *Chem.–Eur. J.*, **13**, 8739 (2007).
- [39] P.Q. Zheng, Y.P. Ren, L.S. Long, R.B. Huang, L.S. Zheng. *Inorg. Chem.*, **44**, 1190 (2005).
- [40] P.M. Forster, A.R. Burbank, C. Livage, G. Férey, A.K. Cheetham. *Chem. Commun.*, 368 (2004).
- [41] I.D. Brown, In *Structure and Bonding in Crystals*, M. O'Keefe, A. Navrotsky (Eds), Vol. 2, pp. 1–30, Academic Press, New York (1981).
- [42] A.I. Minyaev, I.A. Denisov, V.E. Soroko, V.A. Kononov. *Z. Prikl. Khim.*, **59**, 339 (1986).
- [43] T.A. Patterson, J.C. Carver, D.E. Leyden, D.M. Hercules. *J. Phys. Chem.*, **80**, 1702 (1976).
- [44] Y.B. Liu, L.M. Duan, X.M. Yang, J.Q. Xu, Q.B. Zhang, Y.K. Lu, J. Liu. *J. Solid State Chem.*, **179**, 122 (2006).
- [45] O. Kahn. *Molecular Magnetism*, VCH, New York (1993).